Coupled capillary and gravity-driven instability in a liquid film overlying a porous layer

Th. Desaive* and G. Lebon
University of Liège, Institute of Physics, B5, B-4000 Liège, Belgium

M. Hennenberg
Université Libre de Bruxelles, Microgravity Research Center, Caisse Postale 165, 1050 Brussels, Belgium
(Received 5 July 2001; published 21 November 2001)

In this work, we study the problem of onset of thermal convection in a fluid layer overlying a porous layer, the whole system being heated from below. We use Brinkman's model to describe the porous medium and determine the corresponding linear stability equations. The eigenvalue problem is solved by means of a modified Galerkin method. The behavior of the critical wave number and temperature gradient is discussed in terms of the various parameters of the system. We also emphasize the influence of the boundary conditions at the upper surface of the fluid layer; in particular, we examine the role of a free surface whose surface tension is temperature dependent (Marangoni effect). Comparison with earlier works is also made.

DOI: 10.1103/PhysRevE.64.066304 PACS number(s): 47.20.Bp, 47.20.Dr, 44.25.+f, 47.27.Te

I. INTRODUCTION

Thermal convection of fluids in porous media has been extensively investigated [1] since the pioneering work of Horton and Rogers [2] and Lapwood [3], mainly because of its technological importance. The related problem of a composite system, consisting of a liquid layer overlying a porous layer, has received significant attention. This configuration is found in numerous applications such as water reservoirs, postaccident cooling of nuclear reactors [4], and solid matrix heat exchangers. A good review of flow interaction and heat transfer between fluid and porous layers is found in [5]. Nield [6] first formulated the problem of thermal convection in a fluid surmounting a saturated porous medium when the system is bounded by two horizontal heat insulating boundaries. Nield proposed an analytical solution for the problem of a nonoscillatory linear regime and a zero critical wave number. This last assumption was a physical guess based on previous results obtained for thermocapillary instabilities in single-fluid layers between two insulating boundaries (the Rayleigh-Marangoni-Bénard problem) and for thermoconvection in porous media. The two-layer porous medium plus fluid problem sandwiched between two rigid boundaries was studied by Chen and Chen [7] who used Darcy's law to describe the porous layer and the classical slip condition of Beavers and Joseph [8] at the liquid–porous-medium interface. Their linear analysis predicts the existence of a critical depth ratio, i.e., the ratio of the thickness of the fluid layer to that of the porous layer. This critical value characterizes a switch from a dominating circulation in the porous layer to a dominating circulation in the liquid layer. Their numerical results were confirmed experimentally [9] and an extension to the nonlinear regime was found in [10]. Poulikakos [11] used the more general nonlinear Brinkman-Forchheimer model to investigate numerically the characteristics of the flow and temperature fields in a box. Taslim and Narusawa [12] examined extensively the influence of the dimensionless numbers on the critical values in three different configurations of the porous-liquid system.

The present study aims at developing the linear stability analysis of a porous-liquid bilayer system under rather general conditions. Instead of Darcy's law, we use the Brinkman model [13]; the upper fluid boundary is either rigid or free and will include a Marangoni effect. In pure fluid systems, it has been widely recognized since the work of Pearson [14] and Nield [15] that surface tension gradients play a decisive role in the onset of convective instabilities [16,17]. In the presence of a porous medium, this Marangoni effect has received less attention and this has motivated the present study. Other related efforts to solve the problem can be found in the papers by Vasseur *et al.* [18], Hennenberg *et al.* [19], and Rudraiah and Prasad [20]. By comparison with these works, we propose a more complete and systematic linear approach to the problem. In particular, the effect of several dimensionless groups on the critical values is detailed and the influence of the nature of the upper fluid boundary is emphasized.

II. MATHEMATICAL FORMULATION

We consider the configuration formed by an incompressible fluid layer of thickness d_l overlying a homogeneous porous layer of thickness d_p saturated by the same liquid (see Fig. 1). The system is supposed to be of infinite extent in the

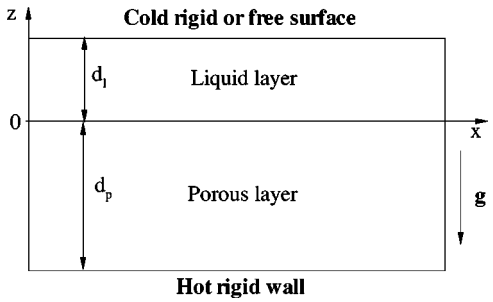

FIG. 1. The geometrical configuration.

*Electronic address: tdesaive@ulg.ac.be

horizontal directions with its density given by the state equation

$$\rho_k = \rho_0[1-\alpha_T(T_k - T_0)], \tag{1}$$

where the subscript k refers to the layer ($k=l$ for the liquid layer or p for the porous medium), ρ_0 is the density of the liquid at temperature T_0, and α_T is the constant coefficient of volumic expansion. The system subject to the gravity field is heated from below and the upper surface of the fluid is either rigid, or free with a linear dependence of the surface tension on temperature:

$$\sigma = \sigma_0 - \gamma(T_l - T_0), \tag{2}$$

where σ_0 is the surface tension of the fluid at temperature T_0 and the constant rate of change of surface tension with temperature, γ, is supposed to be positive. Cartesian coordinates are used with the origin at the interface between the porous medium and the fluid layer and with the z axis vertically upward.

We take for granted Boussinesq's approximation in both layers and assume that the fluid is Newtonian. The continuity, momentum, and energy equations for the fluid layer are respectively given by

$$\nabla \cdot \mathbf{u}_l = 0, \tag{3}$$

$$\rho_0 \partial_t \mathbf{u}_l + \rho_0 \mathbf{u}_l \cdot \nabla \mathbf{u}_l = -\nabla p_l - \rho_0 g[1-\alpha_T(T_l - T_0)]\mathbf{e}_z + \mu_l \nabla^2 \mathbf{u}_l, \tag{4}$$

$$\partial_t T_l + \mathbf{u}_l . \nabla T_l = \kappa_l \nabla^2 T_l, \tag{5}$$

where $\mathbf{u}_l(u_l, v_l, w_l)$ designates the velocity field, p_l the pressure, T_l the temperature, μ_l the dynamic viscosity, k_l the thermal conductivity, c the specific heat at constant pressure, and $\kappa_l = k_l/\rho_0 c$ the thermal diffusivity.

Although Darcy's law is widely used to describe porous media, we prefer to choose the Brinkman model [13] which accounts for friction caused by macroscopic shear. It is known that this effect seriously affects the flow field especially in sparsely packed porous media. This amounts to considering the saturated porous matrix as a specific fluid with an effective viscosity μ_e and subject to an additional external body force, namely, the classical Darcy term. Doing this allows us to keep the main ingredients of a fluid system since we conserve the same mathematical structure as the equations of Newtonian fluid mechanics. The continuity, momentum and energy equations for the porous layer read therefore as

$$\nabla \cdot \mathbf{u}_p = 0, \tag{6}$$

$$\frac{\rho_0}{\phi}\partial_t \mathbf{u}_p + \frac{\rho_0}{\phi^2}\mathbf{u}_p \cdot \nabla \mathbf{u}_p = -\nabla p_p - \rho_0 g[1-\alpha_T(T_p - T_0)]\mathbf{e}_z + \mu_e \nabla^2 \mathbf{u}_p - \frac{\mu_l}{K}\mathbf{u}_p, \tag{7}$$

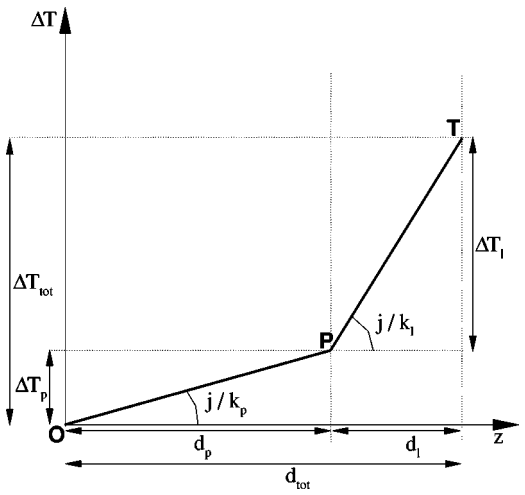

FIG. 2. Scheme of the conductive reference state.

$$(\rho_0 c)_p \partial_t T_p + (\rho_0 c)_l (\mathbf{u}_p \cdot \nabla T_p) = k_p \nabla^2 T_p, \tag{8}$$

wherein ϕ designates the porosity, K the permeability, $\mathbf{u}_p(u_p, v_p, w_p)$ the seepage velocity, p_p the pressure, T_p the temperature, and k_p the mean thermal conductivity in the porous layer. For any physical property one has $(\,)_p = (1-\phi)(\,)_s + \phi(\,)_l$ where the subscript s denotes a property of the solid matrix.

III. SMALL PERTURBATION EQUATIONS AND RELEVANT BOUNDARY CONDITIONS

From now on, we restrict the analysis to the evolution of infinitesimally small perturbations. The governing equations are linearized with respect to the reference state, namely, a motionless fluid with heat transported only by conduction. It is worth stressing that the unperturbed heat flux j crossing the porous-liquid interface is continuous in the conductive rest state and one can write

$$k_l \frac{\Delta T_l}{d_l} = k_p \frac{\Delta T_p}{d_p} = k_{tot} \frac{\Delta T_{tot}}{d_{tot}}, \tag{9}$$

where $k_{tot} = d_{tot}/(d_p/k_p + d_l/k_l)$ is the mean conductivity while the subscript tot refers to the ''total'' system. Figure 2 gives a graphical representation of ΔT_p, ΔT_l, and ΔT_{tot} when the liquid and porous layers have different thermal conductivities. The lines OP and PT represent, respectively, the temperature profiles in the porous and the liquid layers with slopes given by j/k_p and j/k_l as the reference conducting flux j is continuous between both phases.

For convenience, the variables are expressed in dimensionless form and we use one single set of scaling units for the complete system. In particular, the length is scaled by the total thickness $d_{tot} = d_l + d_p$, the temperature by $\Delta T_{tot} = \Delta T_l + \Delta T_p$, the time by d_{tot}^2/κ_l, and the velocity by κ_l/d_{tot}. In this way, we do not single out either of the two phases.

Eliminating the pressure fields, the dimensionless equations for the linearized perturbed variables take the following simplified expressions and involve only four unknown quan-

tities, namely, the vertical component of the velocities in both the fluid and porous layers and the corresponding temperature fields. It is found that

$$\mathrm{Pr}^{-1}\phi^{-1}\partial_t\nabla^2 w_p = \mathrm{Ra}\nabla_h^2 T_p + \Lambda\nabla^4 w_p - \mathrm{Da}^{-1}\nabla^2 w_p, \quad (10)$$

$$\partial_t T_p = S\frac{k_{tot}}{k_p} w_p + SX^{-1}\nabla^2 T_p, \quad (11)$$

$$\mathrm{Pr}^{-1}\partial_t\nabla^2 w_l = \nabla^4 w_l + \mathrm{Ra}\nabla_h^2 T_l, \quad (12)$$

$$\partial_t T_l = \nabla^2 T_l + \frac{k_{tot}}{k_l} w_l, \quad (13)$$

wherein all the symbols refer to dimensionless variables. Six dimensionless parameters have been introduced in the above equations, namely, $\mathrm{Ra}=\alpha_T g\Delta T_{tot} d_{tot}^3/\nu_l\kappa_l$, the Rayleigh number, $\mathrm{Pr}=\mu_l/\rho_0\kappa_l$, the Prandtl number, $\mathrm{Da}=K/d_{tot}^2$, the Darcy number, $\Lambda=\mu_e/\mu_l$, the dynamic viscosity ratio, $X=k_l/k_p$, the thermal conductivity ratio, and $S=(\rho c)_l/(\rho c)_p$, the heat capacity ratio.

In contrast to other authors [6,7], we introduce neither a porous Rayleigh number $\mathrm{Ra}_p=\alpha_T g\Delta T_p d_p K/\nu_l\kappa_p$ nor a liquid Rayleigh number $\mathrm{Ra}_l=\alpha_T g\Delta T_l d_l^3/\nu_l\kappa_l$, as one single set of scaling units is used. It is easily checked that Ra, Ra_p, and Ra_l are related by

$$\mathrm{Ra}_p = \frac{\mathrm{Ra}(1-d)^4}{1-d+dX}, \quad (14)$$

$$\mathrm{Ra}_l = \frac{\mathrm{Ra}\, d^2 X^2\, \mathrm{Da}}{1-d+dX}, \quad (15)$$

where $d=d_p/d_{tot}$. To solve the set (10)–(13), we need 12 boundary conditions, which are given below.

At the lower wall $(z=-d)$ the boundary is assumed rigid and perfectly heat conducting, so that

$$w_p = 0, \quad (16)$$

$$\partial_z w_p = 0, \quad (17)$$

$$T_p = 0. \quad (18)$$

At the interface $(z=0)$. Interfacial conditions express the continuity of the normal and tangential velocities, the continuity of temperature and heat flux, and finally the continuity of the normal and tangential components of the stress tensor. This results in

$$w_p = w_l, \quad (19)$$

$$\partial_z w_p = \partial_z w_l, \quad (20)$$

$$T_p = T_l, \quad (21)$$

$$\partial_z T_p = X\partial_z T_l, \quad (22)$$

$$\Lambda(\partial_z^3 w_p + 3\nabla_h^2\partial_z w_p) - \frac{1}{\mathrm{Da}}\partial_z w_p = \partial_z^3 w_l + 3\nabla_h^2\partial_z w_l, \quad (23)$$

$$\nabla_h^2 w_l - \partial_z^2 w_l = \Lambda(\nabla_h^2 w_p - \partial_z^2 w_p). \quad (24)$$

Boundary conditions (20) and (24) are formulated as a consequence of Brinkman's law; by using Darcy's law, one should have to supply only the Beavers-Joseph condition [8].

At the upper surface $(z=1-d)$. In the linear approach, the validity of Boussinesq's approximation implies that surface deformations are negligible [21,15], so that

$$w_l = 0. \quad (25)$$

Heat transfer is assumed to be governed by Newton's cooling law

$$\partial_z T_l + \mathrm{Bi}\, T_l = 0, \quad (26)$$

wherein Bi is the Biot number. The upper boundary is either rigid, from which it follows that

$$\partial_z w_l = 0, \quad (27)$$

or free with a Marangoni effect, in which case Eq. (27) is replaced by

$$\partial_z^2 w_l - \mathrm{Ma}\,\nabla_h^2 T_l = 0, \quad (28)$$

where $\mathrm{Ma}=\gamma\Delta T_{tot} d_{tot}/\nu_l\kappa_l$ is the Marangoni number.

IV. NORMAL MODE DECOMPOSITION

According to the normal mode technique, we seek solutions for the vertical velocity components and temperature of the form

$$\begin{pmatrix} w_i \\ T_i \end{pmatrix} = \begin{pmatrix} W_i(z) \\ \Theta_i(z) \end{pmatrix} \exp[i(a_x x + a_y y) + st] \quad (29)$$

for each layer i $(i=l,p)$. The amplitudes $W_i(z)$ and $\Theta_i(z)$ describe the variation with respect to z of the vertical velocity and the temperature in each layer, and a_x and a_y are the dimensionless wave numbers in the x and y directions, respectively. Finally, s is the complex growth rate of the disturbances.

The use of Brinkman's model together with the above choice of scaling units suggests the introduction of two of the alternative dimensionless numbers λ and α instead of the classical Ra and Ma numbers. These parameters were first proposed by Parmentier *et al.* [22] and Regnier *et al.* [23] in the case of one-layer systems. The introduction of these parameters is motivated by the fact that α is directly related to the ratio of buoyancy to thermocapillarity while λ is proportional to the temperature difference across the system. Ra and Ma are related to α and λ by means of

$$\mathrm{Ra} = (\mathrm{Ra})_0\alpha\lambda, \quad (30)$$

$$\mathrm{Ma} = (\mathrm{Ma})_0(1-\alpha)\lambda, \quad (31)$$

where $(\mathrm{Ra})_0$ and $(\mathrm{Ma})_0$ are two arbitrary constants chosen here as the critical Rayleigh number for pure buoyancy and the critical Marangoni number for pure thermocapillarity in a liquid layer.

Assuming that the principle of exchange of stability holds (i.e., s is set equal to zero at marginal stability) and introducing the expansion (29) as well as relations (30) and (31) in Eqs. (10)–(13), we obtain

$$\Lambda(D^2-a^2)^2W_p-\mathrm{Da}^{-1}(D^2-a^2)W_p-a^2(\mathrm{Ra})_0\alpha\lambda\,\Theta_p=0, \tag{32}$$

$$(D^2-a^2)\Theta_p+X\frac{k_{tot}}{k_p}W_p=0, \tag{33}$$

$$(D^2-a^2)^2W_l-a^2(\mathrm{Ra})_0\alpha\lambda\,\Theta_l=0, \tag{34}$$

$$(D^2-a^2)\Theta_l+\frac{k_{tot}}{k_l}W_l=0, \tag{35}$$

where D stands for d/dz. The above four equations give rise to a 12th order system with the following associated boundary conditions.

At $z=-d$, one has

$$W_p=0, \tag{36}$$

$$DW_p=0, \tag{37}$$

$$\Theta_p=0. \tag{38}$$

At $z=0$,

$$W_l=W_p, \tag{39}$$

$$DW_l=DW_p, \tag{40}$$

$$\Theta_l=\Theta_p, \tag{41}$$

$$X\,D\Theta_l=D\Theta_p, \tag{42}$$

$$\Lambda(D^3W_p-3a^2DW_p)-\frac{1}{\mathrm{Da}}DW_p=D^3W_l-3a^2DW_l, \tag{43}$$

$$(D^2+a^2)W_l=\Lambda(D^2+a^2)W_p. \tag{44}$$

Finally, at $z=1-d$,

$$W_l=0, \tag{45}$$

$$D\Theta_l+\mathrm{Bi}\,\Theta_l=0, \tag{46}$$

$$D^2W_l+a^2(\mathrm{Ma})_0(1-\alpha)\lambda\,\Theta_l=0. \tag{47}$$

Note that the dimensionless parameters Pr and S have disappeared from the above equations due to the fact that σ was set to zero at marginal stability.

V. RESULTS AND COMMENTS

A. Analytical results for constant-flux thermal boundary conditions

As mentioned in the Introduction, Nield [6] was the first to study the linear stability of a porous-liquid bilayer system sandwiched between two heat insulating boundaries. The zero critical wave number due to these boundary conditions allowed him to derive the stability criterion analytically. Expanding the temperature and the vertical velocity fields as well as the Rayleigh and Marangoni numbers in terms of powers of a^2 and solving the problem at orders a^0 and a^2, one easily obtains the compatibility condition. Assuming that the porous layer is described by the Brinkman model, we extend Nield's method to obtain a relation describing the locus of the critical Rayleigh number Ra_c and the critical Marangoni number Ma_c. This relation has the following generic expression

$$\mathrm{Ra}_c\,f_1(Da,X,d,\Lambda)+\mathrm{Ma}_c\,f_2(Da,X,d,\Lambda)=f_3(Da,X,d,\Lambda), \tag{48}$$

where f_1, f_2, and f_3 are complicated functions of the different parameters of the system. In the particular case $X=1$, Vasseur *et al.* [18] used the parallel flow assumption to obtain an expression similar to Eq. (48). Both Nield's and Vasseur's methods yield the same values of f_1, f_2, and f_3 for different Darcy numbers and depth ratios in the case of insulating boundaries. Here we find it interesting to check relation (48) for some other cases.

1. One single viscous fluid layer between one rigid and one free boundary.

Letting $d\to 0$ and $\mathrm{Da}\to 0$, Eq. (48) becomes

$$\frac{\mathrm{Ra}_c}{320}+\frac{\mathrm{Ma}_c}{48}=1, \tag{49}$$

recovering the classical result of Nield [15].

2. Porous medium with an upper free surface

We let now $d\to 1$, $\mathrm{Ma}\to 0$, and $\Lambda\to 1$. Equation (48) reads

$$\mathrm{Ra}_p^c=\frac{12[-\cosh(1/\sqrt{Da})+\sqrt{Da}\sinh(1/\sqrt{Da})]}{12(1-2\,\mathrm{Da})\mathrm{Da}+(-1+24\,\mathrm{Da}^2)\cosh(1/\sqrt{Da})+4(1-6\,\mathrm{Da})\sqrt{Da}\sinh(1/\sqrt{Da})}, \tag{50}$$

TABLE I. Comparison of the critical conditions for $Da^{Chen}=4\times10^{-6}$ and $X=0.7$

	a_p^c		Ra_p^c	
d	This study	Ref. [7]	This study	Ref. [7]
0.909	2.14	2.14	19.121	19.093
0.901	23.4	23.41	14.743	14.294
0.885	20.03	20.05	7.782	7.535
0.752	8.28	8.29	0.214	0.207

where Ra_p^c is the critical value of the porous Rayleigh number defined in Eq. (14). With Ra_p finite and $Da\rightarrow0$ in Eq. (50), it is found that

$$Ra_p^c=12, \tag{51}$$

which corresponds to the critical value of a Darcy medium between two rigid walls [6]. This conclusion could also have been drawn from Eq. (48) for any value of X.

B. Numerical results for general thermal boundary conditions

We first check our computer code by comparing the critical conditions with those of Chen and Chen [7]. We introduce therefore the porous wave number (a_p) and the porous Rayleigh number (Ra_p) already defined in relation (14). Since the dimensional wave number must be the same in the liquid and porous layers as matching of the solutions in the two layers is required, we have the following relations between the porous wave number a_p, the liquid wave number a_l, and the overall wave number a:

$$\frac{a_l}{d_l}=\frac{a_p}{d_p}=\frac{a}{d_{tot}}. \tag{52}$$

In [7] the upper fluid boundary is rigid and perfectly heat conducting, Darcy's law is selected, and the Beavers-Joseph slip condition [8] is applied at the porous-liquid interface. To solve the 12th order eigenproblem, we use a modified Galerkin method based on a Chebychev polynomial expansion of $W_l(z)$, $W_p(z)$, $\Theta_l(z)$, and $\Theta_p(z)$. Table I shows a comparison between our results and those of Chen and Chen [7] for $Da^{Chen}=4\times10^{-6}$ ($Da^{Chen}=Da/d^2$) and $X=0.7$. A very good accord between both approaches is observed.

The neutral stability curves expressing λ in terms of the wave number a using Brinkman's law are shown in Fig. 3 for different depth ratios d. This figure is qualitatively similar to the stability curves obtained by Chen and Chen [7] with Darcy's model. For large depth ratios, the curves are bimodal, exhibiting two relative minima, and the long-wave branch is the most unstable. For small depth ratios, the short-wave branch is the most unstable. One also observes that, for lower depth ratios, the long-wave instability disappears. To understand the reason for this modal change, we have also represented in Fig. 4 the streamline patterns corresponding to the short-wave (on the left) and long-wave (on the right) modes. The convection is clearly dominated by the porous layer in the long-wave mode but the onset of convection occurs in both the fluid and the porous layers. For the short-wave mode, convection takes place only in the fluid region. Thus, the modal change is the result of switching from a porous-layer dominated circulation to a liquid-layer dominated circulation. These results confirm that Chen and Chen's conlusions [7] remain valid not only for Darcy's but also for Brinkman's law.

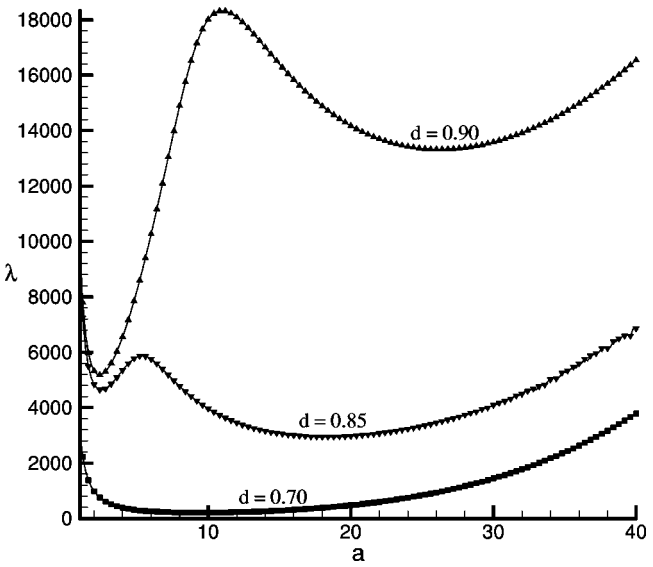

FIG. 3. Neutral stability curves with Brinkman's law.

As already pointed out in Sec. II, Brinkman's model rests on an effective viscosity μ_e denoted Λ in dimensionless form. Most published works based on Brinkman's model assume $\mu_e=\mu_l$ [24,25] which means $\Lambda=1$, but recently Givler and Altobelli [26] determined experimentally that $\Lambda=7.5^{+3.4}_{-2.4}$ for wall-bounded flow through a cylindrical plug of porous material. Because of this important difference in the values of Λ, we found it interesting to study the influence of this parameter on the critical values. Figure 5 shows the variation of a_c and λ_c with the parameter Λ. Globally, Λ has a minor effect on the critical wave number a_c which runs from 27.6 (for $\Lambda=1$) to 28.4 (for $\Lambda=20$), but Λ has a more sensitive influence on λ_c. It is interesting to note that the

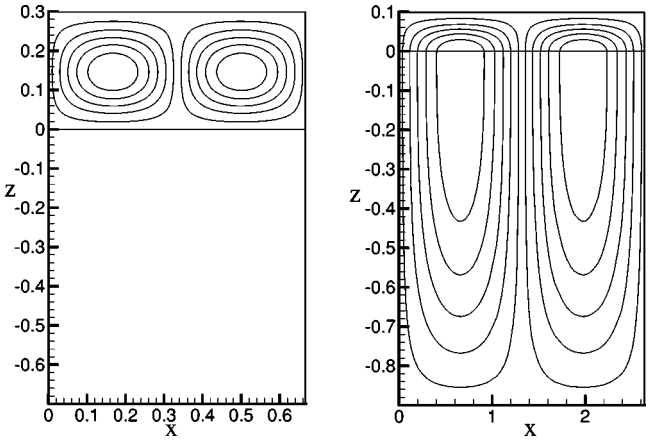

FIG. 4. Streamline patterns with Brinkman's law. $Da=10^{-5}$, $X=0.7$, $Bi=\infty$, and $d=0.7$ (on the left) and 0.9 (on the right).

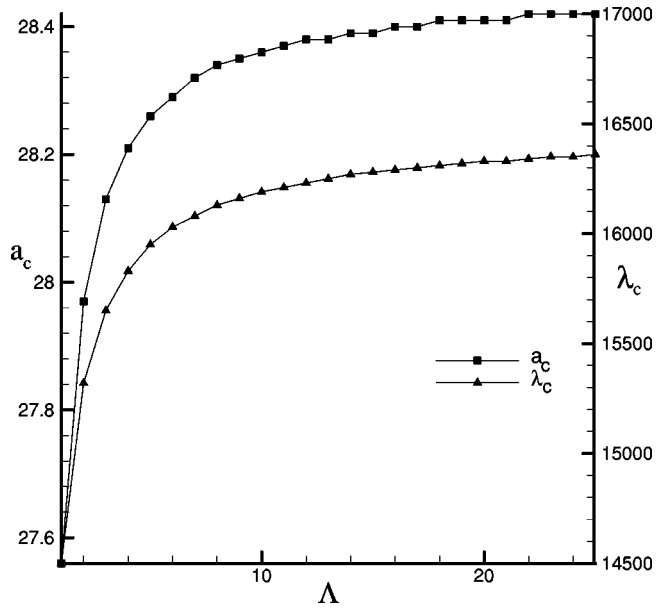

FIG. 5. Effect of the viscosity ratio Λ on the critical wave number a_c and the critical temperature difference λ_c ($\mathrm{Da}=10^{-5}$, $X=0.7$, $\mathrm{Bi}=\infty$, and $d=0.9$).

critical values remain quasiconstant for Λ greater than 10. For simplicity, we will take $\Lambda=1$ in the following as its value has no determining influence on the critical conditions.

It was mentioned above that the stability curves are generally bimodal and that a modal change is observed when changing the depth ratio. This phenomenon was first described by Chen and Chen [7] for Darcy's model but for only one value of their Darcy number, namely, $\mathrm{Da}^{Chen}=9\times10^{-6}$. Here, we want to complement the result of Chen and Chen by examining the influence of the Darcy number on the switch between porous dominated and liquid dominated circulation as a function of d. Figure 6 shows the effect of the

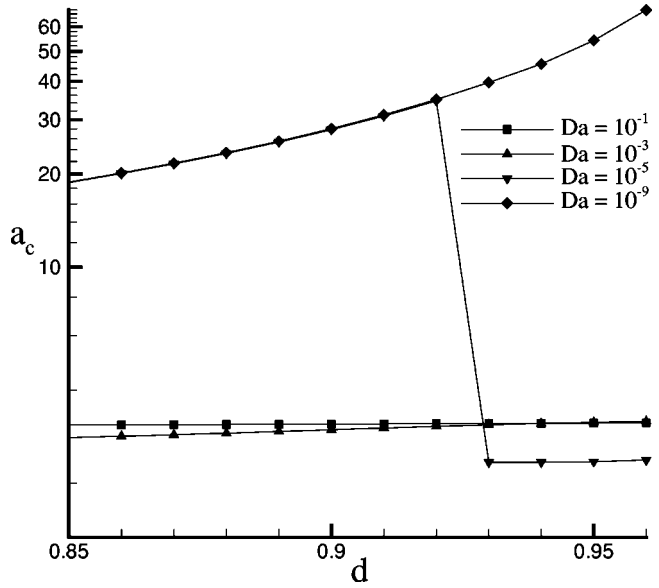

FIG. 6. Effect of Darcy number Da on the critical wave number as a function of d ($X=0.7$ and $\mathrm{Bi}=\infty$).

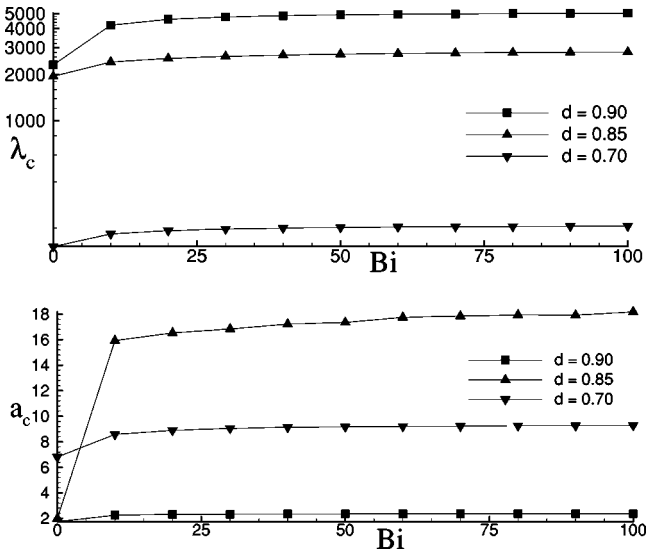

FIG. 7. Effect of Bi on a_c and λ_c in the pure buoyancy case ($\alpha=1$, $X=0.7$, and $\mathrm{Da}=10^{-5}$).

depth ratio on the critical wave number for four values of Da. For $\mathrm{Da}=10^{-6}$, we observe a sudden jump in the critical wave number around $d=0.93$ from the short-wave mode to the long-wave mode but there is no jump in the other curves. One notices that the short-wave branch is absent for small values of Da, which corresponds to a not very permeable porous medium. Hence, as the porous layer strongly dampens the penetration of the fluid, the circulation is maintained in the fluid layer (the long-wave mode). For large values of Da, the short-wave branch is absent, as could have been expected because the very permeable porous layer no longer dampens the fluid motion and convection is observed in the whole cavity. The bilayer system behaves more like a fluid and $a_c\simeq3.1$, which is the critical value observed in a pure liquid between two rigid isothermal walls.

VI. INFLUENCE OF THE TOP BOUNDARY CONDITIONS ON THE CRITICAL VALUES

A first linear stability analysis of thermoconvection in a porous-liquid bilayer was done by Nield [6] who studied the situation of two layers bounded by rigid adiabatically insulating walls. Chen and Chen [7], Taslim and Narusawa [12], and Poulikakos [11] considered rigid perfectly heat conducting walls. The originality of our approach is that we investigate the more general case of a top boundary that can be either rigid or free, including a Marangoni effect; moreover, we use Newton's cooling law (Biot condition) as a more general thermal condition.

The effect of the Biot number on the critical values is shown in Fig. 7 for pure buoyancy and for several depth ratios. Figure 7 indicates that the variation of Bi from 0 to 10 significantly affects the magnitude of a_c and λ_c. For higher values of Bi, the role of Bi is minute. This behavior is not surprising as the nature of the boundary changes drastically from an insulated surface to a partially conductive boundary. It is clear that, on increasing the Biot number, temperature perturbations will not grow so easily, therefore increasing the

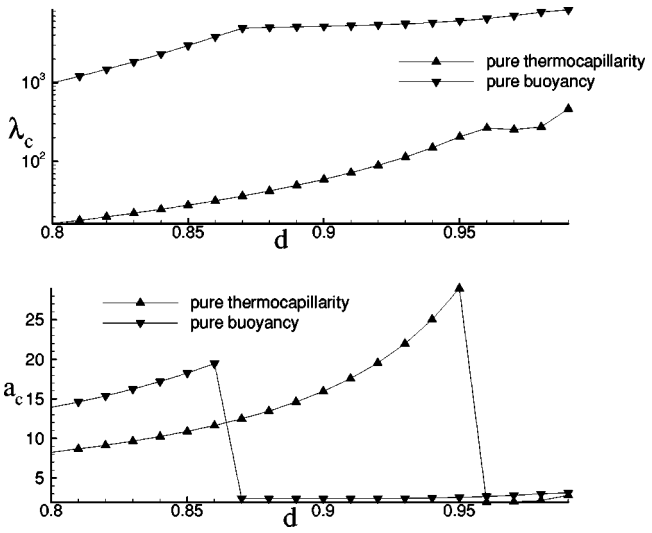

FIG. 8. Effect of α on a_c and λ_c ($\mathrm{Da}=1\times10^{-5}$ and $X=0.7$). $\alpha=0$, pure capillarity; $\alpha=1$, pure buoyancy.

critical temperature gradient. When the Biot number becomes larger and larger, more energy is required to induce motion and it is also natural that the critical wavelength of the convective cells decreases. Figure 7 thus provides an *a posteriori* justification of the infinite Biot number used in the previous simulations since the critical values are nearly independent of Bi.

To analyze the influence of the Marangoni condition, we have plotted in Fig. 8 the critical values a_c and λ_c for two values of the parameter α that measures the relative importance of the capillary and buoyancy effects. The curves in Fig. 8 show the evolution of a_c and λ_c with the depth ratios in the pure buoyancy case ($\alpha=1$) and in the pure thermocapillary case ($\alpha=0$). We first observe that capillarity is more destabilizing than buoyancy as the critical values λ_c are larger for $\alpha=1$ than for $\alpha=0$. The critical depth ratio corresponding to the transition from a liquid-layer dominated circulation to a porous-layer dominated circulation is much larger for $\alpha=0$ than for $\alpha=1$. Therefore the appearance of large cells extending over both layers is restricted to a very small fluid depth in the pure thermocapillary case. By comparison, the convection cells are larger in the thermocapillary case than in the buoyancy case because the corresponding wave numbers are smaller. The difference in the sizes of the cells tends to decrease for the long-wave mode, i.e., for a_c tending to zero.

VII. CONCLUSIONS

A linear stability analysis is proposed to study the onset of thermal convection in a porous medium underlying a liquid layer, the system being heated from below. With respect to previous works, we have examined the effects resulting from the substitution of Darcy's by Brinkman's law. We have also given up the assumption of a rigid upper boundary, either perfectly heat conducting or heat insulating. We have investigated the more general situation wherein the upper boundary of the fluid layer is free with a temperature dependent surface tension; moreover, heat transfer is described by the more general Newton cooling law with Biot number varying between zero and infinity.

The main results obtained can be summarized as follows. First, it is shown that Brinkman's model gives qualitatively the same results as Darcy's law. Indeed, the effective viscosity introduced in Brinkman's approach does not significantly affect the critical stability conditions. Second, the stability curves are bimodal for large depth ratios and one observes a sudden jump in the critical wave number when the depth ratio is modified, as already reported by Chen and Chen [7]. In addition, the critical depth ratio disappears at very large and at very small Darcy numbers. Third, we have emphasized the influence of the upper boundary condition in the liquid layer. In the pure thermocapillary case convection is confined to the fluid layer except for a very small fluid depth. This result is interesting as it opens the possibility of stopping undesirable convection in the porous medium. In work now in progress, we will examine whether the presence of a porous support will modify the nature of the patterns appearing in the fluid layer. This will be achieved in the framework of a nonlinear approach based on the amplitude method.

ACKNOWLEDGMENTS

This text presents results of the Belgian Program Inter-University Pole of Attraction (IUPA 5) initiated by the Belgian State, Prime Minister's Office, Federal Office for Scientific, Technical and Cultural Affairs. Support from ESA through the CIMEX-MAP project and from the European Union through the ICOPAC project (Contract No. HRPN-CT-2000-00136) is also acknowledged. It is also a pleasure to thank Dr. J. Bragard for stimulating discussions as well as Professor E. Arquis and Professor J. P. Caltagirone (MASTER Laboratory, ENSCPB, Bordeaux).

[1] D.A. Nield, *Convection in Porous Media*, 2nd ed. (Springer-Verlag, Berlin, 1999).
[2] C.W. Horton and G.T. Rogers, J. Appl. Phys. **16**, 367 (1945).
[3] E.R. Lapwood, Proc. Cambridge Philos. Soc. **44**, 508 (1948).
[4] C.W. Somerton and I. Catton, J. Heat Transfer **104**, 160 (1982).
[5] V. Prasad, in *Convective Heat and Mass Transfer in Porous Media*, edited by S. Kakaç, B. Kilkis, F.A. Kulacki, and F. Arinç (Kluwer Academic, Dordrecht, 1991), pp. 563–615.
[6] D.A. Nield, J. Fluid Mech. **81**, 513 (1977).
[7] F. Chen and C.F. Chen, J. Heat Transfer **110**, 403 (1988).
[8] G.S. Beavers and D.J. Joseph, J. Fluid Mech. **30**, 197 (1967).
[9] F. Chen and C.F. Chen, J. Fluid Mech. **207**, 311 (1989).
[10] F. Chen and C.F. Chen, J. Fluid Mech. **234**, 97 (1992).
[11] D. Poulikakos, Phys. Fluids **29**, 3949 (1986).
[12] M.E. Taslim and U. Narusawa, J. Heat Transfer **111**, 357

(1989).
[13] H.C. Brinkman, Appl. Sci. Res., Sect. A **1**, 27 (1947).
[14] J.R.A. Pearson, J. Fluid Mech. **4**, 489 (1958).
[15] D.A. Nield, J. Fluid Mech. **9**, 341352 (1964).
[16] P. Colinet, J.C. Legros, and M.G. Velarde, *Nonlinear Dynamics of Surface Tension Driven Instabilities* (Wiley-VCH, Berlin, 2001).
[17] E.L. Koschmieder, *Bénard Cells and Taylor Vortices* (Cambridge University Press, Cambridge, 1993).
[18] P. Vasseur, C.H. Wang, and M. Sen, Waerme Stoffuebertrag. **24**, 337 (1989).
[19] M. Hennenberg, M.Z. Saghir, A. Rednikov, and J.C. Legros, Transp. Porous Media **27**, 327 (1997).
[20] N. Rudraiah and V. Prasad, Acta Mech. **127**, 235 (1998).
[21] S.H. Davis and L.A. Segel, Phys. Fluids **11**, 470 (1968).
[22] P.M. Parmentier, V.C. Regnier, G. Lebon, and J.C. Legros, Phys. Rev. E **54**, 411 (1996).
[23] V. Regnier, P.C. Dauby, P. Parmentier, and G. Lebon, Phys. Rev. E **55**, 6860 (1997).
[24] T.S. Lundgren, J. Fluid Mech. **51**, 273 (1972).
[25] G. Neale and W. Nader, Can. J. Chem. Eng. **52**, 475 (1974).
[26] R.C. Givler and S.A. Altobelli, J. Fluid Mech. **258**, 355 (1994).